E-proceedings of the 36th IAHR World Congress
28 June – 3 July, 2015, The Hague, the Netherlands

3D NUMERICAL MODELLING OF NEAR BED FLOW OVER AN ARTIFICIAL GRAVEL BED

VINCENZO SESSA[(1)], NILS RÜTHER[(2)] & CARLO GUALTIERI[(1)]

[(1)] *Civil, Construction and Environmental Engineering Department (DICEA), University of Napoli "Federico II", Napoli (Italy). E-mail: vincen.sessa@gmail.com; carlo.gualtieri@unina.it*

[(2)] *Department of Hydraulic and Environmental Engineering, Norwegian University of Science and Technology (NTNU), Trondheim (Norway). E-mail: nils.ruther@ntnu.no*

ABSTRACT

The understanding of flow structures over static armor layers is essential for the development of modern sediment transport models. Over a rough boundary, such as in a gravel bed channel, friction created by individual gravel bed particles or cluster of particles retards the flow velocity creating near-bed turbulence, which plays an important role in the dynamics of a river. Very recently, the use of an artificial gravel bed in river engineering studies has proved to be highly advantageous for the investigation of steady flow and for a more easy comparison with the results obtained elsewhere. The present paper investigated the possibility to simulate the flow over an artificial gravel bed. The numerical results were compared with the experimental data collected in a physical model by Spiller et al. (2013) using Particle Image Velocimetry (PIV). The commercial code STAR-CCM+ was chosen to simulate the flow over the gravel bed. The flow was calculated by solving the Reynolds-Averaged Navier-Stokes equations in combination with the standard k-ε model. The free surface was simulated by the Volume-of-fluid method. Five different discharges were chosen from PIV measurements and simulated to see whether the numerical model could reproduce the general and detailed flow characteristics. The numerical results for the streamwise component of the velocity were in good agreement with the experimental data. In particular, the match was very good for the velocities above the roughness height. Whereas within the roughness height the simulated results tended to deviate from the measured ones. The numerical model tended to overestimate the physical one indicating a percentage error between 4% and 7.5% and lower accuracy near the bottom. In general it was observed that with an increasing simulated discharge, the deviation of the velocities increased due to grid resolution. The gravel bed created within STAR-CCM+ lost the perfect roundness of those elements: the larger was the base size chosen for grid, the smoother was the bed and the effects were more visible with higher velocities.

Keywords: river engineering, sediment transport, artificial gravel bed, computation fluid dynamics , RANS equations.

1. INTRODUCTION

Open-channels made up of simple geometry and free of obstructions are desirable for efficient water conveyance. Nowadays, roughness elements, such as gravels, are commonly deployed into artificial open-channels to stabilize the channel sectional shapes and to maintain the ecological balance there. Consequently, the hydrodynamic behavior of flows in these channels is significantly affected. The determination of the velocity and turbulence intensity profiles, as well as the hydraulic resistance, is of practical importance in the engineering design of these channels. One purpose of this study was to quantify the gravel roughness effects on flows and mixing using both experimental and numerical methods. The experiment conducted by Spiller et al. (2013) focused on velocity profiles and turbulent characteristics in a fully rough, uniform channel flow over an artificial gravel bed. One of the major challenges of that experiment was to establish the same prerequisite conditions for every experiment, so that their results could be directly compared. In any movable bed the conditions will change over time and even a static armor layer which should theoretically retain its surface structure will eventually experience some surface rearrangements, especially in case of high flows or highly unsteady flow. An artificial, rigid streambed is fixed and will therefore provide the same precondition for each experiment. Due to bed topography small scale heterogeneity, the flow was not uniform locally in the near-bed region and a double averaging methodology has been applied.

The modeling work was based on the available 3D surfaces and refined them into steady flow models in STAR-CCM+. Particular attention was on grid generation procedures, as this turned out to be a major factor in achieving good results. For the physical setup the numerical modeling was based on solving the RANS equations using a k-ε model. The central part of this work was the comparison between the modeling results and the data coming from the physical model test conducted by Spiller et al. (2013).

2. PAST EXPERIMENTAL WORK

2.1 Artificial streambed

In order to produce a surface structure as close to a real gravel bed as possible, an armor layer developed in a laboratory flume at the Leichtweiß-Institute for Hydraulic Engineering in Braunschweig (Germany) was molded. Using a liquid two-component silicone rubber for the mold, a negative imprint of the streambed could be manufactured. Subsequently, a two-component pouring resin forms an almost exact copy of the original bed structure (Spiller et al. 2013 a&b). The silicone form could be reused to produce several similar streambed copies. A photographic line-by-number-analysis of the original armor layer provides a grain-size distribution with a geometric mean diameter of 13.50 mm. (Figure 1)

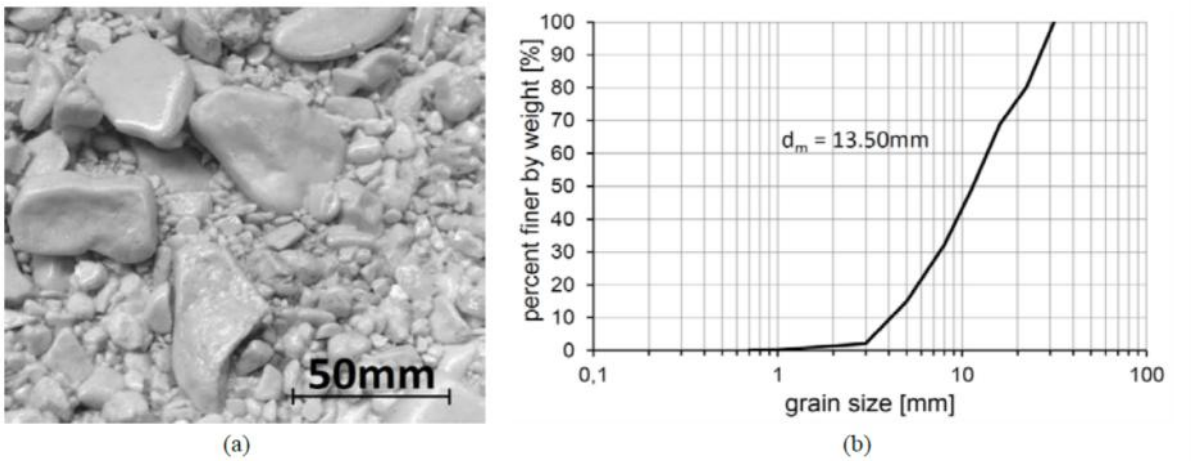

Figure 1. Grain size distribution

2.2 Experimental setup and PIV

The original armor layer was produced in a 30 cm wide, straight laboratory flume with an effective sediment length of 5.35 m. It developed under a constant discharge of 28.9 l/s with a mean bed slope of 5.3 ‰. An exact copy of the original armor layer was moved from the Leichtweiß-Institute for Hydraulic Engineering in Braunschweig (Germany), to the Department of Marine Technology at NTNU in Trondheim (Norway).The experiments were carried out in a non-tilting straight hydraulic flume with a total length of 6.63 m. The central acrylic test section measured 2.50 m in length and 60.9 cm in width. The artificial streambed was installed within the test section. It covered the full width of the flume over a length of 1.60 m in stream wise direction. The stereoscopic Particle Image Velocimetry system used for the experiments consisted of two CCD cameras, positioned on either side of the flume like indicated in Figure 2. In this 15 Hz system, each camera took 15 double frame pictures per second so that the final amount of pictures to process was 60 images per second (Spiller et al. 2013a).

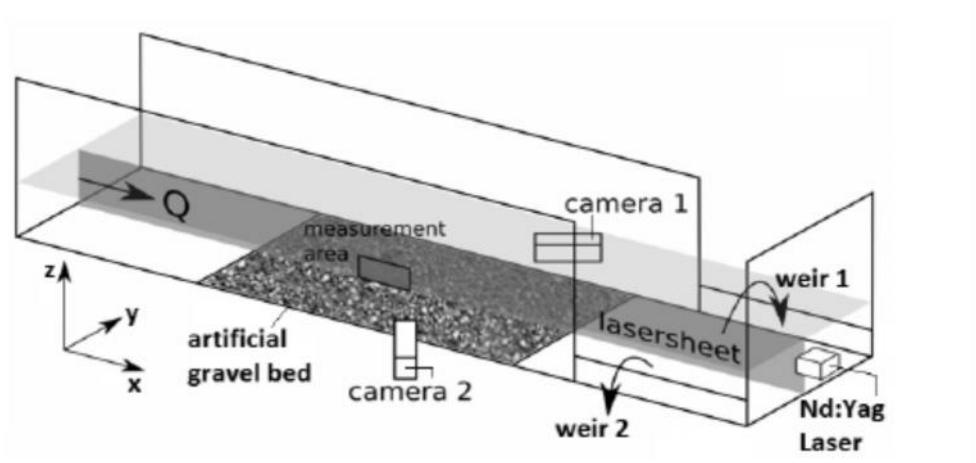

Figure 2. Experiment setup

The experiment was divided into a number of 18 runs. Setting the pump frequency to 5 Hz, a water discharge of 6 l/s evolved. From there, the pump frequency was increased by 1 Hz for each run so that a higher discharge developed in the system. After setting up each run, at least ten minutes passed before the measurements were taken so that the new flow situation could develop and steady conditions in the whole system were reached. After that, some test pictures were taken to determine the optimal pulse distance for the PIV measurement. Since several experimental runs of different discharges

between Q = 6 l/s and Q = 90 l/s were recorded and compared, the mean velocity for each run was different. To maintain an average displacement of about four to six pixels, the pulse distance of the double frame recordings was adjusted for each run. It varied from 13000 µs for the 6 l/s run to 1500 µs for the 90 l/s run (Table 1). Each run was measured over a total time of 40 seconds, resulting in 2400 single images and therefore 600 vector fields for further analysis (Spiller et al. 2013a).

Table 1 shows all 18 runs, each with its discharge, flow depth and chosen pulse distance for the PIV measurement. Figure 3 shows the double averaged (Nikora et al. 2007) streamwise velocity profiles <ū> for each run. The mean velocity was averaged on time and along x-direction within the PIV area. Making spatially averaged profiles of time averaged velocity revealed the spatial variation in the time-averaged flow, and made it possible to chart the form-induced velocity components. In Figure 3 the calculated velocity increased with the discharge. This figure also includes the roughness geometry function in the bottom right corner. The dashed line marks the elevation of the roughness tops.

Table 1. Experimental runs

Q (l/s)	d (mm)	Pulse distance (µm)
6	134	13000
8	137	10000
10	139	8000
13	141	6800
16	146	5800
18	149	5000
21	151	4500
25	155	4200
29	160	3500
36	165	2500
42	171	2200
49	179	2200
56	183	2000
63	191	1900
71	195	1800
77	201	1700
84	204	1600
90	207	1500

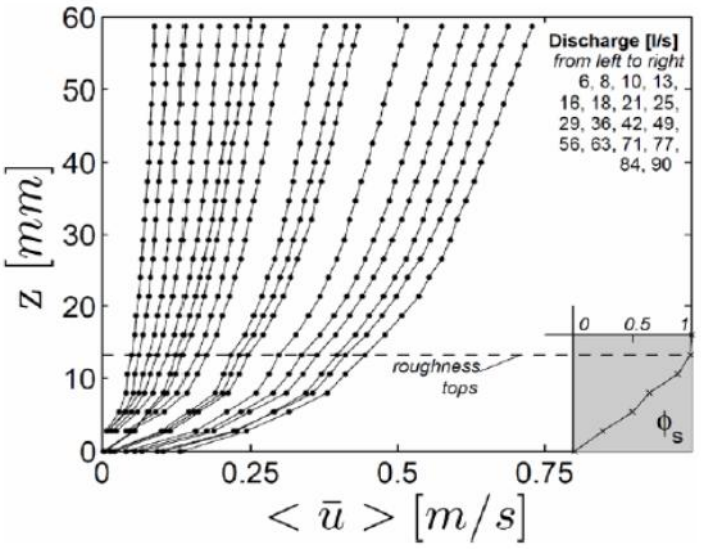

Figure 3. Double averaged velocity profile s in x-direction.

3. NUMERICAL MODEL

3.1 PHYSICAL SETUP

The Reynolds-Averaged Navier-Stokes equations in combination with the k-ε model was solved since the wall effects were not so important. The standard k-ε model was chosen because it is widely used turbulence model that have shown good results in many cases for natural rivers and open channels, e.g. Fisher-Antz et al. (2008), Rüther et al. (2010). The k–ε model is the most widely used turbulence model also because of its ease in implementation, economy in computation and, most importantly, for being able to obtain reasonable accurate solution with the available computer power (Ingham and Ma 2005). However, several shortcomings have been discovered over three decades of use and validation. In open channel flows modeling, it is known that in the case of prismatic channels where there are no geometrical variations along the channel, the k–ε turbulence model fails to predict any evidence of secondary flow. This is because the k–ε model assumes that the turbulence is isotropic, whereas turbulence is known to be anisotropic. In fact, it is the anisotropic behavior of turbulence as it approaches the walls and free surface, namely the imbalance in the normal Reynolds stresses, that creates secondary circulation even if in a straight channel (Knight et al. 2005). Also, the assumption of isotropy, can lead the k–ε model to predict large turbulent viscosity and, consequently, high turbulent diffusivities. Nevertheless, recent studies demonstrated that for simplified cases, where mean velocities and bulk mixing properties are needed, RANS-modeling of shallow flows is still appropriate (Van Prooijen and Uijttewaal 2005; Gualtieri 2010).

A second order upwind discretization was set because it is known to give more accurate results than the first order scheme as in Rüther et al. (2010) In order to compare the numerical results using different turbulent models, the Spalart-Allmaras Turbulence model was used as well. Among all different turbulent models offered by STAR-CCM+, the Spalart and Allmaras turbulence model was chosen just for comparison. The Spalart and Allmaras model was implemented by many groups providing good results in a wide range of different applications. Nevertheless thebe behavior of this new turbulence model is little known. Table 4 sums up the numerical model characteristics. The Eulerian Multiphase was chosen for modeling two different fluids coexisting in each run. The VOF (Volume Of Fluid method) was implemented for modeling the free surface between air and water (Hirt et al. 1981).

Table 4. Numerical model characteristics

Numerical Model characteristics					
Physical Parameters		**Flow conditions**		**Turbulence models**	
Space	Three dimensional	Eulerian Multiphase	Air (ideal gas)	RANS equation	Standard k-ε (2nd order)
			Water		
Time	Implicit Unsteady	Segregated flow	Segregated fluid isothermal	Spallart-Allmaras	Convection (2nd order)
T ρ	300°K 999,97 Kg/m^3	Water surface treatment	VOF		

3.2 MESH

Since the experimental data reported values along cross section each 3 mm from bottom and up to 60 mm, 3 mm mesh size was used in the area of analysis. In order to validate the model as well as to have more data to be compared, 5 mm mesh size was used as well. In Table 5 the two meshes in details.

Table 5. Mesh details

MESH SIZE	**MESH A (5 mm)**	**MESH B (3 mm)**
Cell count	1.099.102	2.254.221
Face count	3.241.699	6.601.113
Base size	20.0 mm	20.0 mm
Prism Layer Thickness	5.0 mm	5.0 mm
Surface Growth Rate	1.3	1.3
Surface size	Relative minimum size 20 mm	Relative minimum size 20 mm
	Relative Target size 20 mm	Relative Target size 20 mm
Volumetric control (Trimmer Anisotropic size)	X 12 mm Y 12 mm Z 5 mm	X 10 mm Y 10 mm Z 3 mm

3.3 NUMERICAL RUNS

Numerical model simulated five different discharges from the experimental data, as shown in Table 6. Reynolds Averaged Navier Stokes equations in combination with the Standard k-ε turbulence model were used for all the runs while the Spalart-Allmaras turbulence model was used for 21 l/s water discharge. Mesh B was used for all the simulations; for 42 l/s water discharge, mesh B was used as well.

Table 6. Numerical runs

Run N°	**Discharge Q (l/s)**	**Depth d (mm)**	**Turbulence model**	**Reynolds number**	**Froude number**
1B	6	134	RANS and k-ε	10537	0.061
2B	21	151	RANS and k-ε	40711	0.197
3B	42	171	RANS and k-ε	80602	0.332
3A	42	171	RANS and k-ε	80602	0.332
4B	63	191	RANS and k-ε	115865	0.395
5B	90	207	RANS and k-ε	174405	0.53
6B	21	151	Spalart-Allmaras	40711	0.197

3.4 POST-PROCESSING

Once each simulation was done as well as all the stopping criteria satisfied, the first step was to verify the model. In order to do this a mass flow plot was created for inspection. A mass flow monitoring on top region was carried out as well, to take into account any water leaks (Pedersen 2013).
Even for validation, the residuals plot was examined, ensuring all the parameters down a certain value with a steady trend. In order to compare the simulation results with the experimental data, the zero point was located near the bottom considering the roughness tops matching at 13.3 mm. Afterwards, in the same area of PIV measurements, a longitudinal grid was positioned.

4. NUMERICAL RESULTS

In the experiment the field of view measured 282 mm in x-direction, meaning along the central streamline and 61 mm in the vertically oriented z-direction, so that, a grid of 20x20 points along x-direction was created. This longitudinal grid of 300x60 mm was located just in the middle of the channel (30 cm from left/right side). In Figure 4 the area of PIV measurements and the related modeling area within STAR-CCM+.

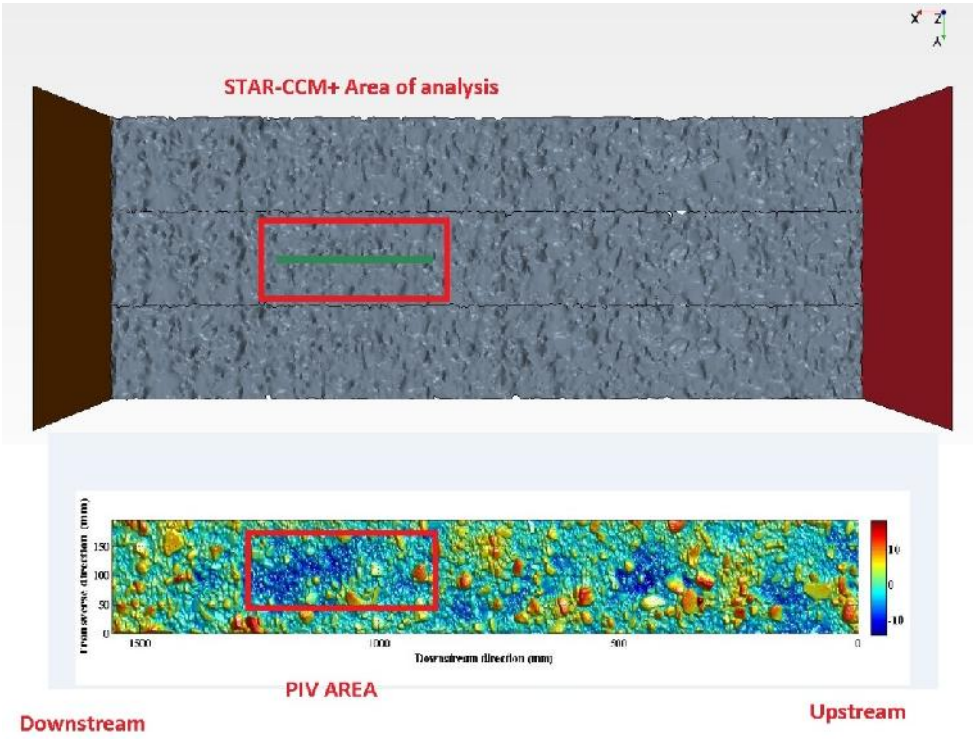

Figure 4. Area of analysis

Once the PIV area was located inside the geometry, the next step was to fix the zero point along z-direction to properly match the numerical velocity profiles and the experimental data. In order to do this the roughness tops elevation was considered the major parameter for matching. In Figure 5 the exact location of zero point.

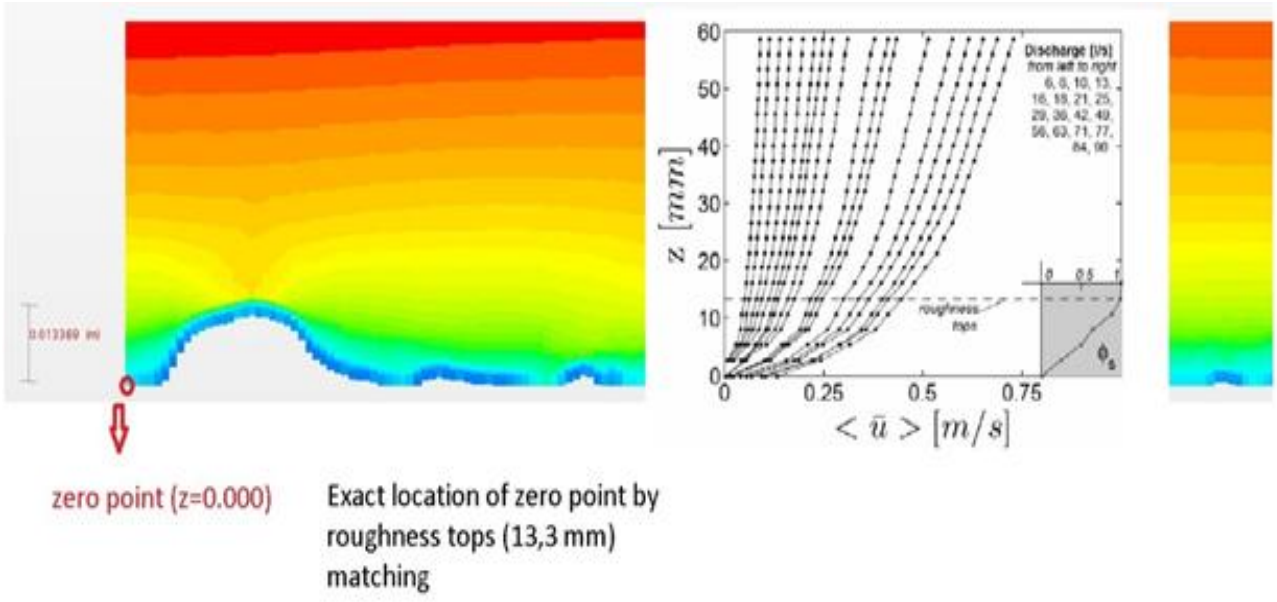

Figure 5. Location of zero point

4.1 MESH COMPARISON

Two different mesh sizes were used during this research, 3 mm mesh size represented the best solution considering the accuracy of the experimental data. In Figure 6 is presented a comparison between the two meshes used for the evaluation of velocity profile in relation to 42 l/s up to 60 mm from bottom. The plot is dimensional: the elevation from bottom in y-direction and the double averaged velocity in x-direction.

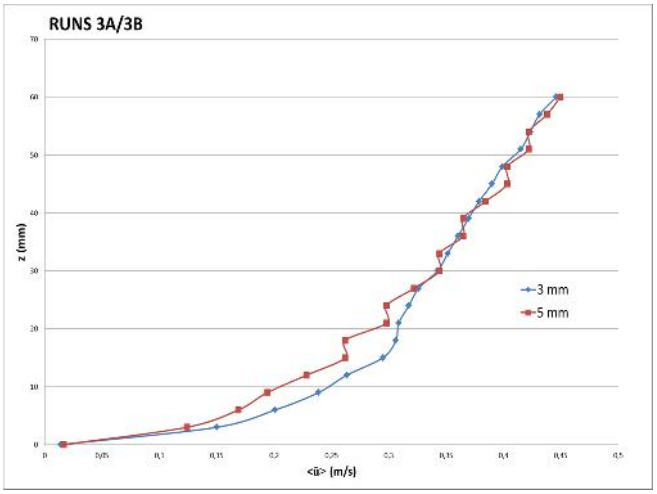

Figure 6. Mesh comparison RUNS 3A/3B

4.2 TURBULENT MODELS IN COMPARISON

Two different turbulent models were simulated for 21 l/s water discharge. Besides RANS equations and k-ε turbulence model, the Spalart-Allmaras turbulence model was chosen to understand which one could be more appropriate for this particular study. So that, in evaluating the accuracy of these two models, numerical and experimental results are plotted and compared in the following figures. The plots are non-dimensional: the elevation on depth from bottom in z-direction, the double averaged velocity on inlet velocity in x-direction.

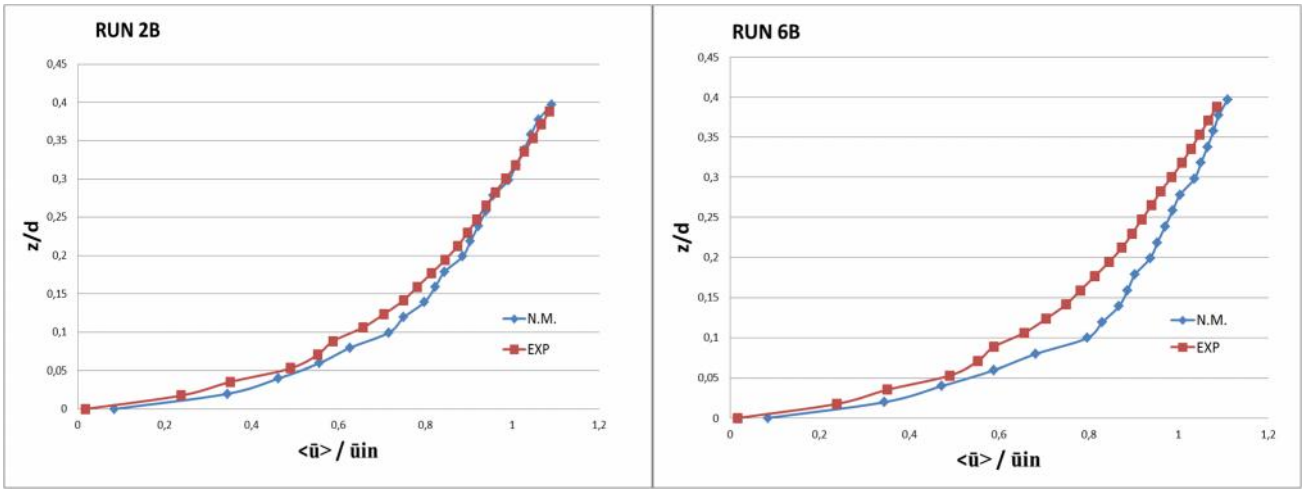

Figure 7. *Left*: RANS and k-ε turbulence model RUN 2B; *right:* Spalart-Allmaras turbulence model RUN 6B

4.3 EXPERIMENTAL DATA COMPARISON

The results of numerical simulations are presented in the following figures. In non-dimensional plots the matching between numerical results and experimental data is showed for 6, 21, 42, 63 and 90 l/s respectively.

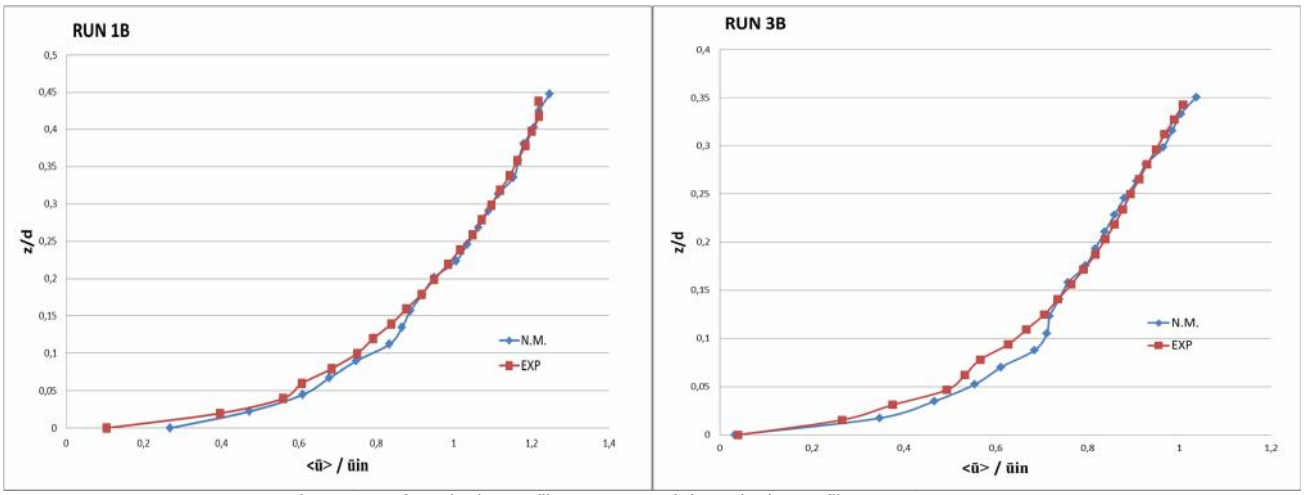

Figure 8. *Left:* Velocity profile RUN 1B; *right:* velocity profile RUN 3B

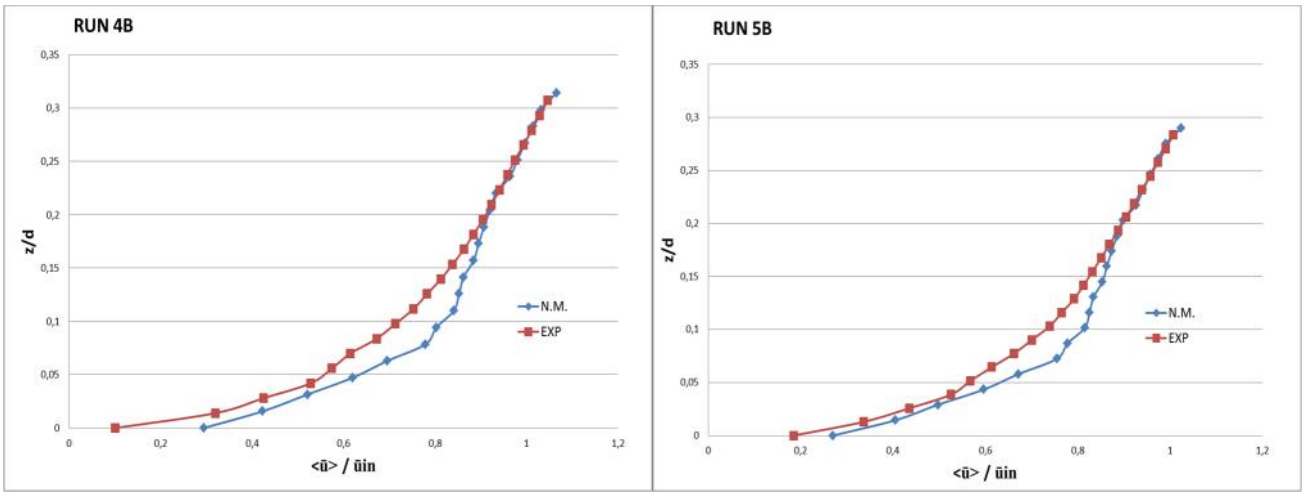

Figure 9. *Left*: Velocity profile RUN 4B; *right:* velocity profile RUN 5B

4.4 NUMERICAL MODEL ACCURACY

In Figure 10 the numerical results are presented in form of average error in relation to the experimental data. The average error is the major parameter in the evaluation of the accuracy of the model.

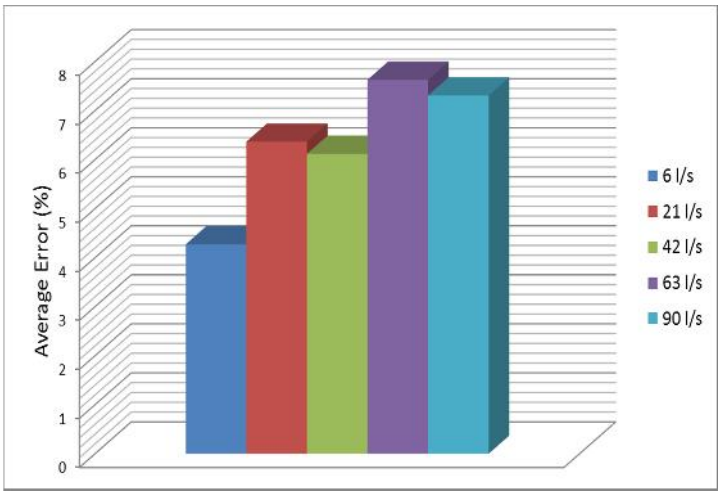

Figure 10. Numerical model accuracy

5. DISCUSSION

The numerical results for the streamwise component of the velocity were in good agreement with the experimental data. In particular, the match was very good for the velocities above the roughness height. Whereas within the roughness height the simulated results tended to deviate from the measured ones. The numerical model tended to overestimate the physical one indicating a percentage error between 4% and 7.5% and lower accuracy near the bottom. In general it was observed that with an increasing simulated discharge, the deviation of the velocities increased due to grid resolution. The gravel bed created within STAR-CCM+ lost the perfect roundness of those elements: the larger was the base size chosen for grid, the smoother was the bed and the effects were more visible with higher velocities. Looking at mesh comparison, it was easy to understand why the 3 mm mesh size was the best solution in spite the two curves were very close. The coarse mesh presented a particular trend because of longitudinal grid size where the data was taken from: considering a cell of 5 mm, there were two same values every three millimeters since they were taken in the same cell. Further, the 3 mm mesh size was much closer to a realistic velocity profile for free surface flow. Looking at the Turbulent model comparison, the Standard k-ε model was very accurate above 0.15 (elevation/depth), while below, quite close. Differently the Spalart-Allmaras seemed to be not able to properly match the experimental data in the area of analysis.

6. CONCLUSION

Numerical methods seem to be most suitable ways of analyzing fluid mechanic problems which give important insights to model turbulent flow. As a suggestion, one is to choose the simplest model which gives acceptable engineering results for the application analyzed: it's always recommended to start with the k-ε turbulence model. More generally, the k–ε model may be recommended for a quick preliminary estimation of the flow field, or in situations where modeling other physical phenomena, such as chemical reactions, combustion, radiation, multi-phase interactions, brings in uncertainties that overweigh those inherent in the k–ε model itself (Hanjalic 2004).
In this research the commercial code STAR-CCM+ was chosen to simulate the flow over an artificial gravel bed. The flow was calculated by solving the Reynolds-Averaged Navier-Stokes equations in combination with the standard k-ε model. The Spalart-Allmaras turbulent model was used for comparison. In the numerical model five different discharges were chosen from a physical model test conducted by Spiller et al. (2013) and simulated. The free surface was simulated by the Volume-of-Fluid method while the Eulerian Multiphase was chosen for modeling two different fluids. Two meshes were used to see whether the numerical model could better reproduce the flow characteristics. The numerical results were compared with the experimental data in form of plots as well as in form of average error in order to estimate the accuracy of the model.

ACKNOWLEDGMENTS

This research was supported by "*Lifelong Learning Programme (LLP) Erasmus 2013/2014*" between the University of Naples *Federico I*I and the Department of Hydraulic and Environmental Engineering of NTNU in Trondheim (Norway). The support and encouragement of Stephan Spiller and Kari Bratveit is gratefully acknowledged.

REFERENCES

Fischer-Antze, T., Olsen, N., & Gutknecht, D. (2008). *Three-dimensional CFD modeling of morphological bed changes in the Danube river*. Water Resources Research, VOL 44.

Gualtieri, C. (2010). *RANS-based simulation of transverse turbulent mixing in a 2D geometry*. Environmental Fluid Mechanics, vol.10, n.1−2, April 2010, pp.137−156.

Hanjalic K. (2004) *Closure models for incompressible turbulent flows*. Lecture Notes at Von Kármán Institute, p 75

Hirt, C., & Nichols, B. (1981). *Volume of Fluid (VOF) Method for the Dynamics of Free Boundaries*. Journal of computational physics 39, 201-225.

Ingham, D.B., Ma, L. (2005) *Fundamental equations for CFD river flow simulations*. In: Bates PD, Lane SN, Ferguson RI (eds) Computational fluid dynamics. Applications in environmental hydraulics. Wiley, Chichester, England, p 534. ISBN 978-0-470-84359-8.

Knight, D.W., Wright, N.G., Morvan, H.P. (2005) *Guidelines for Applying Commercial CFD Software to Open Channel Flow.* Report based on research work conducted under EPSRC Grants GR/R43716/01 and GR/R43723/01, p 31

Nikora, V. et al. (2007). *Double-Averaging Concept for Rough-Bed Open-Channel and Overland Flows: Theoretical Background*. Journal of Hydraulic Engineering, Vol. 133, No. 8, August 2007, pp. 873-883

Pedersen, (2012). *3D Numerical Modelling of Hydropeaking Scenarios in Norwegian Regulated Rivers*. Norwegian University of Science and Technology, Norway, 2012.

Rüther, N., Jakobsen, J., Olsen, N., & Vatne, G. (2010). *Prediction of three dimensional flow field and bed shear stress in a regulated river in Mid-Norway*. Hydrology research, 41.2, 145-152.

Spiller, S., Ruther, N. & Baumann (2013a). *PIV Measurements of Steady Flow over an Artificial Static Armor Layer.* Department of Marine Technology at NTNU in Trondheim, Norway, 2013.

Spiller, S., Ruther, N. & Baumann (2013b). *ARTIFICIAL REPRODUCTION OF THE SURFACE STRUCTURE IN A GRAVEL BED*, Department of Marine Technology at NTNU in Trondheim, Norway, 2013.

Van Prooijen, B.C, Uijttewaal, W.S.J. (2005*) Horizontal mixing in shallow flows*. In: Czernuszenko W., Rowinski, P. (eds) Water quality hazards and dispersion of pollutants. Springer Science+Business Inc., New York, NY, USA, p 250. ISBN 0-387-23321-0.